Focusing surface phonon-polaritons for tunable thermal radiation

Jose Ordonez-Miranda, Masahiro Nomura, Sebastian Volz

Discover Nano

Research

Focusing surface phonon-polaritons for tunable thermal radiation

Jose Ordonez-Miranda[1,2,3] · **Masahiro Nomura**[1,2] · **Sebastian Volz**[1,2]

Received: 21 October 2024 / Accepted: 16 January 2025
Published online: 24 January 2025

Abstract
We demonstrate unprecedented control and enhancement of thermal radiation using subwavelength conical membranes of silicon nitride. Based on fluctuational electrodynamics, we find that the focusing of surface phonon-polaritons along these membranes enhances their far-field thermal conductance by three orders of magnitude over the blackbody limit. Our calculations reveal a non-monotonic dependence of the thermal conductance on membrane geometry, with a characteristic radiation plateau emerging at small front widths due to competing effects of the polariton focusing and radiative area. The obtained results thus introduce the conical geometry as a powerful degree of freedom for tailoring thermal radiation, with potential implications for energy harvesting and thermal management at the nanoscale.

1 Introduction

Thermal radiation through vacuum gaps has attracted significant interest of physicists for several decades [1], due to its potential applications to energy conversion, passive radiative cooling, and thermal management. The near-field radiation between polar dielectric materials (i.e. silicon nitride (SiN) and silicon dioxide (SiO_2)) is characterized by a narrow spectrum of photons and can exceed the conventional Planck's predictions by several orders of magnitude [2–6]. This substantial enhancement is attributed to the coupling between the evanescent waves of surface electromagnetic modes appearing on the radiating surfaces. These surface waves are called Surface Phonon-Polaritons (SPhPs) and can travel distances of a few millimeters at infrared frequencies that are relevant for room temperature applications.

An experimental study [7] of the far-field thermal radiation showed that the blackbody limit can also be overcome by more than 100 times with subwavelength membranes of SiN. This significant increase is driven by the SPhP propagation along the top and bottom surfaces of the membranes and also exists in the near-field regime [8]. Higher radiation rates were observed for hotter and thinner membranes, which represents the fingerprints of the SPhP contribution. Recently, Tachikawa et al. [9] showed that the coating of two microscopic silicon plates with nanometric layers of SiO_2 doubles their far-field thermal radiation. This two-fold enhancement results from the hybridization of SPhPs in SiO_2 with cavity modes in silicon and is well predicted by fluctuational electrodynamics. Therefore, the excitation and in-plane propagation of SPhPs along nanomembranes or microstructures coated with polar nanolayers enhance their thermal radiation, even in the far-field regime. As the propagation of SPhPs along a conical membrane focuses their energy [10–13], the radiation rates between two conical membranes are expected to be even higher than the ones reported for rectangular structures in previous works [7–9]. However, the SPhP contribution to the thermal radiation between two subwavelength conical membranes has not been explored yet, despite its potential to focus and enhance radiative heat currents.

✉ Jose Ordonez-Miranda, jose.ordonez@cnrs.fr | [1]LIMMS, CNRS-IIS IRL 2820, The University of Tokyo, Tokyo 153-8505, Japan. [2]Institute of Industrial Science, The University of Tokyo, Tokyo 153-8505, Japan. [3]Sorbonne Université, CNRS, Institut des Nanosciences de Paris, INSP, F-75005 Paris, France.

In this work, we use fluctuational electrodynamics to study the thermal radiation between two subwavelength conical membranes supporting the propagation of SPhPs. The focusing of these energy carriers propagating along the top and bottom surfaces of the membranes increases their far-field radiative thermal conductance, which is enhanced even more in the near-field regime driven by the coupling of polaritons on the cross-plane surfaces. As the area of these radiating front surfaces scales down, the in-plane focusing of SPhPs increases, while their cross-plane coupling weakens, causing the thermal conductance to reduce until reaching a mininum plateau. This enhancement and plateau are determined by the conicalness of the SiN membranes, as they are not present for rectangular membranes [6–8].

2 Theoretical methodology

Let us consider two conical membranes of SiN exchanging heat by thermal radiation due to their temperature difference ΔT, as shown in Fig. 1. The lateral dimensions $(l, a) = (40, 20)\mu$m of the identical membranes were chosen big enough to ensure a sizable heat exchange and small enough to keep the calculations tractable. These dimensions are also expected to ensure the mechanical stability of the conical membranes, as similar dimensions were used to experimentally probe the far-field radiation between rectangular membranes of SiN [7]. The subwavelength membranes are sufficiently thin ($t = 100$nm) to support the in-plane propagation of SPhPs [7, 14]. The separation distance was fixed at $d = 20\ \mu$m to secure the regime of far-field radiation ($d > \lambda_{th}$) above room temperature. The uniform temperature of each membrane generates the internal fluctuation of electromagnetic currents, whose energy emission generate thermal radiation. According to fluctuational electrodynamics, the net radiative heat flux between the membranes is given by [15, 16]

$$q = \int_0^\infty \hbar\omega\left[f_\omega(T + \Delta T) - f_\omega(T)\right]\Phi(\omega)d\omega, \tag{1}$$

where ω is the radiation frequency, $f_\omega(T) = \left[\exp\left(\hbar\omega/k_B T\right) - 1\right]^{-1}$ is the Bose–Einstein distribution function, $\hbar$ and k_B are the respective reduced Planck and Boltzmann constants, and Φ is the transmission function of the energy emitted from the left membrane (emitter) into the right one (receiver). We determine Φ by using the boundary-element method, a sophisticated formulation in which the electromagnetic fields are calculated from the fluctuations of surface currents [16]. The predictions of this method have been validated by abundant experimental data obtained for the near-field and far-field thermal radiation [7–9], and we used it here via the free software solver Scuff-EM. For the sake of simplicity and conciseness, we evaluate q through the thermal conductance $G = q/\Delta T$, which for a temperature difference $\Delta T \ll T$ and the linear approximation of $f_\omega(T + \Delta T) \approx f_\omega(T) + \Delta T\,\partial f_\omega(T)/\partial T$, becomes independent of ΔT and is determined by

$$G = \int_0^\infty \hbar\omega\frac{\partial f_\omega(T)}{\partial T}\Phi(\omega)d\omega. \tag{2}$$

The Scuff-EM calculations were done by assuming that the environment is in thermal equilibrium with the cold membrane and discretizing both membranes into surface elements, as shown in Fig. 2a. The meshing was chosen sufficiently fine to generate 30,408 fluctuational surface currents, which ensure the transmission function convergence for frequencies up to 40 THz that are relevant for our thermal conductance calculations. All calculations were done for SiN membranes,

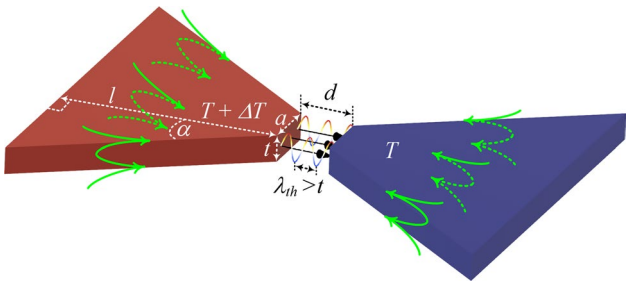

Fig. 1 Scheme of two conical membranes exchanging thermal radiation through photons (wavy lines) and SPhPs (green lines). The photons are emitted from the facing surfaces, while the SPhPs are radiated after propagating along the top and bottom surfaces. The membranes are identical and their red and blue colors indicate high ($T + \Delta T$) and low (T) temperature, respectively. The thickness t is smaller than the Wien's wavelength λ_{th}, which is around 10 μm at 300 K. Black arrows represent the direction of the total heat flux

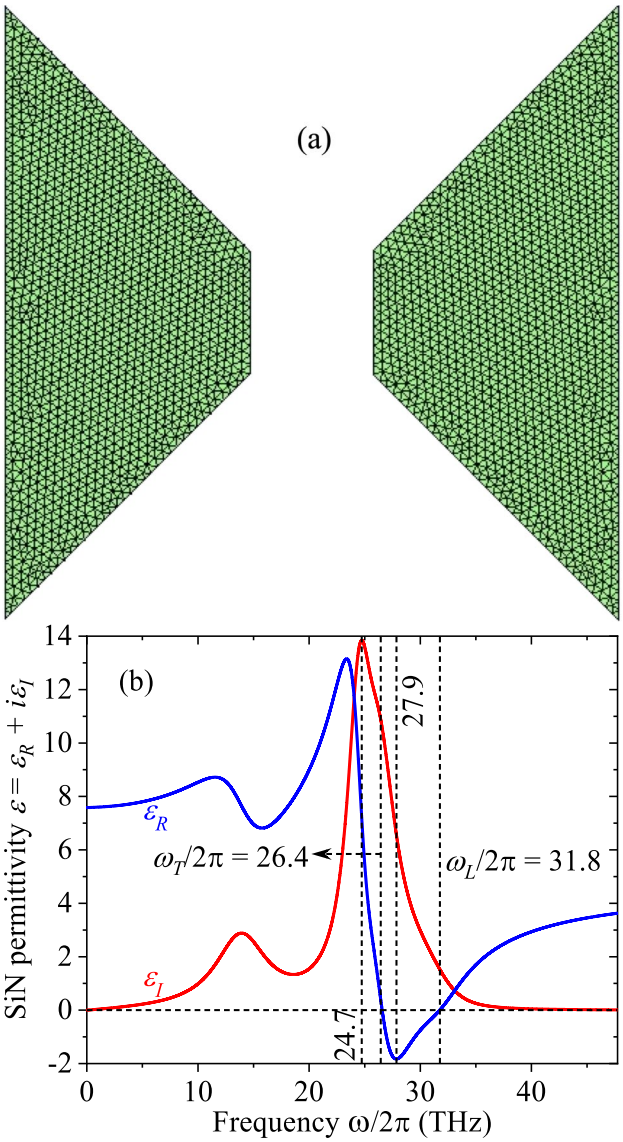

Fig. 2 **a** Surface mesh generated for the Scuff-EM calculations and **c** real and imaginary parts of the relative permittivity of SiN as functions of frequency [17]. Calculations in (**a**) were done for $\alpha = 45°$ and the main transverse optical (ω_T) and longitudinal optical (ω_L) phonon frequencies of SiN are highlighted in (**b**) for reference

which are good SPhP conductors widely used in previous studies [7, 8, 17]. Further, the frequency spectrum of the real and imaginary parts of the SiN permittivity $\varepsilon = \varepsilon_R + i\varepsilon_I$ required for the determination of Φ are shown in Fig. 2b. Our previous measurements showed that this complex property of SiN is, in practice, independent of temperature (for $T < 800$K) and thickness (for $t > 30$nm) [17]. The relatively narrow peak of ε_I and negative dip of ε_R indicate that SiN absorbs energy and favors the SPhP propagation in short frequency intervals, respectively. The thermal excitation and propagation of SPhPs in SiN membranes are thus expected to enhance the radiative heat transfer via their energy emission at the membranes' boundaries.

3 Results and discussion

The spectral transmission function Φ between two SiN conical membranes is shown in Fig. 3a for four aperture angles. For rectangular membranes ($\alpha = 0°$), Φ exhibits a relatively narrow peak ($\sim 20 - 30$ THz) centered at 23.9 THz, which nearly coincides with the frequency of maximum absorption of the SiN permittivity shown in Fig. 2b. This

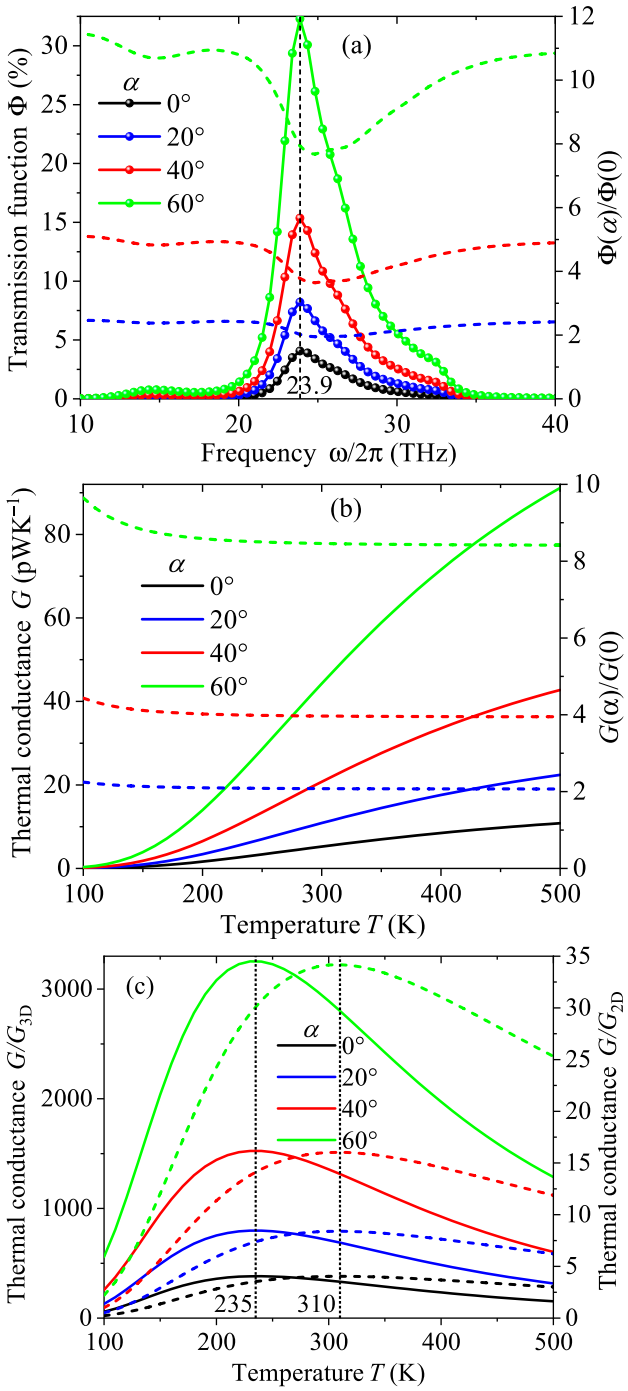

Fig. 3 **a** Frequency spectrum of the transmission function between two SiN conical membranes. **b** Temperature evolution of the thermal conductance and **c** its normalized values with respect to the 3D (solid lines) and 2D (dashed lines) thermal conductances predicted by Eqs. (3a) and (3b) for blackbodies

coincidence is reasonable given that a good energy absorber is also a good emitter, as established by Kirchhoff's law of thermal radiation [18]. The peak frequency of Φ does not change with the aperture angle, whose increase generates higher transmission functions spanning wider frequency intervals. The ratio $\Phi(\alpha)/\Phi(0)$ increases with α through a nonlinear dependence on frequency due to the widening of the Φ peak. This enhancement of Φ leads to a significant increase of the thermal conductance G with α, as shown in Fig. 3b. Higher G values are obtained for wider and hotter membranes, such that $G(\alpha = 60°) > 8G(\alpha = 0°)$. Note that the ratio $G(\alpha)/G(0) \approx \Phi(\alpha)/\Phi(0)$ increases with α and is practically independent of temperature, for $T > 200$ K. This behavior indicates that the focusing effect

driven by the aperture angle acts like a multiplying factor $F(\alpha) > 1$ enhancing $G(\alpha) = F(\alpha)G(0)$. A direct numerical comparison between $G(\alpha)/G(0)$ and the ratio of cross-section area $A(\alpha)/A(0) = 1 + 2(l/a)\tan(\alpha)$ for a conical membrane, indicates that this factor $F(\alpha) \approx 1 + 2(l/a)\tan(\alpha)$. Therefore, the enhancement of the far-field thermal radiation increases with the aperture angle α because of the increment of the cross-plane $[A(\alpha)/A(0) = 1 + 2(l/a)\tan(\alpha)]$ and in-plane $[S(\alpha)/S(0) = 1 + (l/a)\tan(\alpha)]$ areas that support the energy emission of photons and SPhPs, respectively. Keeping in mind that the emission of the SPhP energy at the boundaries of rectangular membranes enhances G beyond the blackbody limit [7, 9], the SPhPs are also expected to increase the far-field radiation between conical membranes beyond this limit.

Figure 3c shows that the increase of G with α leads to radiation rates much greater than the following three-dimensional (3D) or two-dimensional (2D) thermal conductance of two blackbody membranes [19]

$$G_{3D} = 4adF_{12}\sigma_{3D}T^3, \tag{3a}$$

$$G_{2D} = 3aF_{12}\sigma_{2D}T^2, \tag{3b}$$

where $\sigma_{3D} = 2\pi^5 k_B^4/(15c^2 h^3) = 5.67 \cdot 10^{-8}\ \mathrm{Wm^{-2}K^{-4}}$ and $\sigma_{2D} = 8z(3)k_B^3/(ch^2) = 1.92 \cdot 10^{-10}\ \mathrm{Wm^{-1}K^{-3}}$ are the 3D and 2D Stefan-Boltzmann constants, and F_{12} is the geometrical view factor for two rectangular surfaces of cross-plane area at and minimum separation distance d. Considering the finite thickness of the membranes and the purely geometrical nature of F_{12}, its values are common for Eqs. (3a) and (3b), as done in previous works [19, 20]. The temperature dependence of G_{3D} and G_{2D} arises from a 3D and 2D density of photon states, respectively; and therefore, it represents the fingerprint of the dimensionality of the thermal radiation. Note that the thousand-fold enhancement of G over G_{3D} is one order of magnitude higher than the one obtained for rectangular membranes [7] and takes its maximum value for $T = 235$ K. This peak temperature is independent of the aperture angle, whose increase leads to higher ratios G/G_{3D}. The comparison of the transmission function shown in Fig. 3a with the one for two 3D blackbodies $\Phi_{3D} = AF_{12}(\omega/2\pi c)^2$ monotonically increasing with frequency, indicates that the peak temperature of G/G_{3D} is generated by the peak and bounded spectrum of Φ. This transmission peak at 23.7 THz gives rise to a narrow peak on the spectral thermal conductance at the same frequency, which does not change with temperature. By contrast, the unbounded behavior of Φ_{3D} generates a spectral thermal conductance with a peak frequency increasing with temperature, as established by the Wien's displacement law [18]. Therefore, the absence and presence of the displacement of this peak frequency with the temperature of the respective SiN membranes and blackbodies induces the peak exhibited by G/G_{3D}. This fact is confirmed by Fig. 4a, which shows that the monotonic increase of G with α strengthens for temperatures close to the peak temperature $T = 235$ K. Note that this increase accelerates for $\alpha > 50°$, which confirms the great potential of the aperture angle of conical membranes to enhance their thermal radiation. On the other hand, the values of G/G_{2D} are two orders of magnitude smaller than the corresponding ones of G/G_{3D}, but its behavior with temperature and aperture angle is similar and exhibits a peak at 310 K. Hence, the far-field thermal radiation enhancement over the two blackbody limits can be tuned through the temperature and aperture angle of conical membranes to reach values much higher than the ones reported for rectangular ones [7, 8, 21]. Further, the radiation rate also increases with the membranes' thickness, as shown in Fig. 4b. For a given angle and temperature, the thermal conductance increases by a factor between 2 and 3, when the thickness t doubles. This behavior is explained by the fact that the thermal radiation increases not only with the emission cross-section area (at), but also with the view factor ($\sim t$) and in-plane emission of the conical membranes. Importantly, the proximity of the thermal conductance values $G(d = 100\ \mathrm{nm},\ T = 500\ \mathrm{K}) \approx G(d = 200\ \mathrm{nm},\ T = 300\ \mathrm{K})$ and $G(d = 50\ \mathrm{nm},\ T = 500\ \mathrm{K}) \approx G(d = 100\ \mathrm{nm},\ T = 300\ \mathrm{K})$ indicates that the reduction of the radiation rates at lower temperature can be overcome with thicker membranes. The thickness and temperature thus play equivalent roles on the far-field thermal radiation.

Considering that the SiN membranes support not only the cross-plane emission of photons but also the in-plane propagation of SPhPs, we analyze the impact of these latter energy carriers on the obtained thermal conductance via the spatial distribution of the Poynting vector magnitude shown in Fig. 5 around the radiating surfaces of two rectangular ($\alpha = 0$) and conical ($\alpha = 45°$ and $60°$) membranes. Note that the energy density is distributed along the interfaces of the left membranes (emitters), mainly in the immediate proximity outside their boundaries. This energy confinement along the surface of the membranes confirms the significant contribution of SPhPs to increase the cross-section area of the

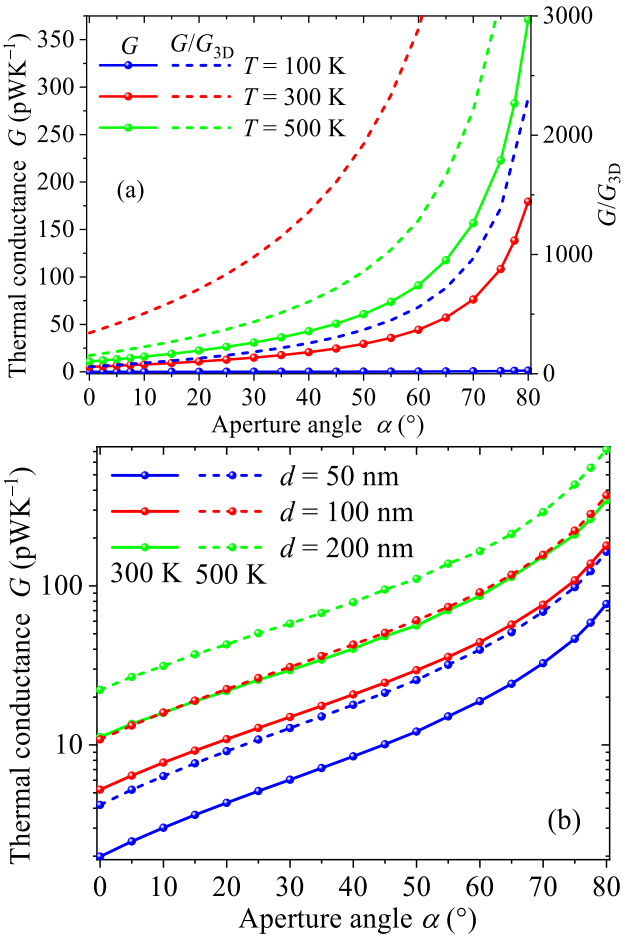

Fig. 4 Thermal conductance between two SiN conical membranes as a function of their aperture angle, for a thickness of **a** $d = 100$nm and **b** $d = 50,\ 100,\ 200$nm. Calculations were done for representative temperatures

membranes and therefore to enhance their far-field thermal radiation beyond the blackbody limit. According to Figs. 2b and 3a, this enhancement results from frequencies supporting the in-plane propagation of SPhPs, which indicates that the increased cross-section is correlated to a large density of polariton states, in agreement with previous works for rectangular membranes [7, 20]. Note that the left conical membranes confine more energy than its rectangular counterpart and hence generates a stronger and longer emission of energy toward the right membrane (receiver). Larger cross-section areas and longer distances of energy emission are obtained for bigger aperture angles. Therefore, the conical membranes make better use of the SPhP energy than the rectangular ones to enhance their far-field thermal radiation.

Figures 6a,b show that the thermal conductance between conical membranes can also be enhanced by reducing their separation distance d to the nanoscale and increasing their width a, respectively. The increase of G does not saturate and becomes particularly significant for $d < 1$ µm and $a > 1$ µm due to the increasing near-field effects and geometrical cross-section area (at). This fact indicates that the near-field coupling of SPhPs appearing on the cross-plane surfaces strengthens the thermal radiation despite their relatively small area with respect to the in-plane surface area (A(cross-plane)$/A$(in-plane) $= (t/l)\left[a/l + 2\tan(\alpha)\right]/\left[a/l + \tan(\alpha)\right]$). Therefore, a small enough separation distance allows to exploit the SPhPs to enhance the thermal radiation between subwavelength membranes, in spite of their relatively small thickness. When the temperature is raised from 300 to 500 K, this enhancement becomes independent of the separation distance in the extreme near-field ($d < 20$ nm) and far-field ($d > 10$ µm) regimes, as shown by the dashed line in Fig. 6a. A higher ratio $G(500\text{K})/G(300\text{K})$ is obtained for smaller gaps, as the near-field thermal energy generated by SPhPs increases with temperature [8, 17, 19]. This conductance ratio is also nearly independent of the membranes' width due to the plateau of G for $a < 1$ µm, as shown in Fig. 6b. This saturation of the thermal conductance for small enough front

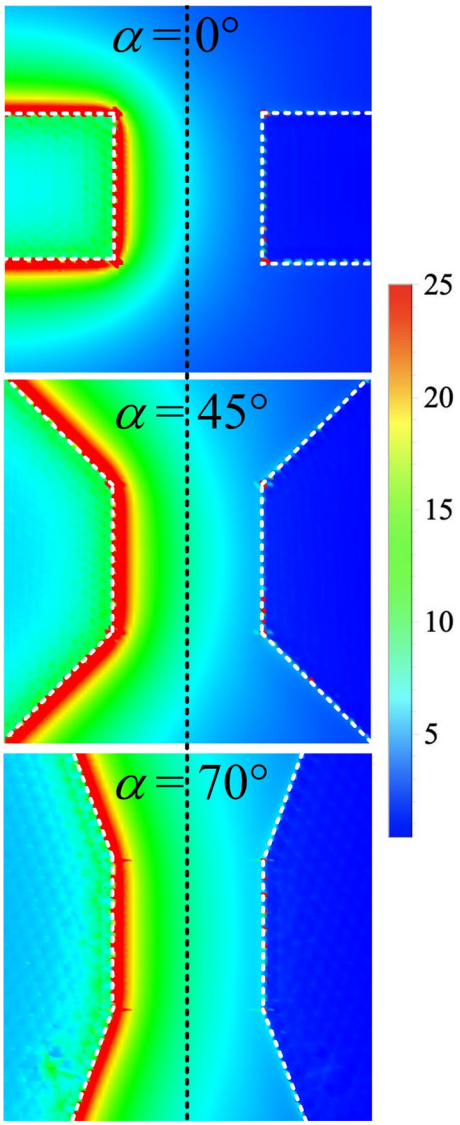

Fig. 5 Density map of the Poynting vector magnitude between two SiN membranes with an aperture angle of **a** 0°, **b** 45°, and **c** 70°. Calculations were done for the bottom surface ($z = 0$) of the membranes and the peak frequency $\omega/2\pi = 23.9$ THz of the transmission function shown in Fig. 3a. The black dashed line represents the system center. The conical left membranes emits their energy longer distances than the rectangular left membrane

widths is generated by the balance between the focusing of the in-plane propagation of SPhPs and the reduction of the cross-plane area $a \times t$ radiating their energy. The conicalness of the membranes thus enhances their thermal radiation, provided that their front width is sufficiently long to support a significant emission of the SPhP energy.

4 Conclusions

Based on fluctuational electrodynamics, we have determined the thermal radiation rates between two subwavelength conical membranes of silicon nitride supporting the in-plane and cross-plane propagation of surface phonon-polaritons. The obtained far-field thermal conductance increases with the membranes' aperture angle, is greater than the corresponding one predicted for rectangular membranes, and is mainly described by the increase of the radiating surface area. Compared with the blackbody limit, we have observed a 1000-fold enhancement in the far-field thermal radiation between two 100-nm-thick membranes with a separation gap of 20 μm. This significant enhancement takes its maximum for temperatures around 235 K. Higher thermal conductances are obtained for smaller gaps and greater widths of the radiating surfaces. By contrast, as the width of these front surfaces scales down, the increasing focusing of polaritons is

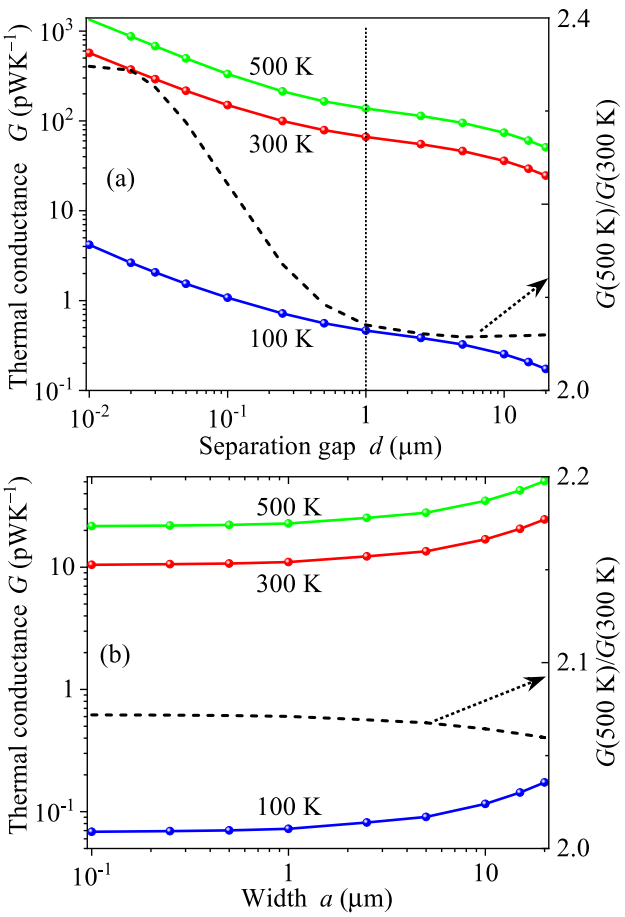

Fig. 6 Thermal conductance between two SiN conical membranes as a function of their **a** separation distance and **b** width. The dashed line represents the ratio $G(500\ \mathrm{K})/G(300\ \mathrm{K})$. Calculations were done for an aperture angle $\alpha = 45°$, three representative temperatures, a width $a = 20\ \mu\mathrm{m}$ in (**a**) and a gap $d = 20\ \mu\mathrm{m}$ in (**b**)

offset by the reduction of the cross-plane area supporting the thermal emission, which generates a minimum plateau for the far-field thermal conductance. Our findings thus reveal the great potential of surface phonon-polaritons to enhance and control the far-field and near-field radiation between conical membranes.

Acknowledgements We thank Roman Anufriev for his valuable contribution to implementing the Scuff-EM simulations. This work was supported by the CREST JST (N° JPMJCR19I1) and KAKENHI JSPS (NN° 21H04635) projects.

Data availibility The datasets generated during and/or analyzed during the current study are available from the corresponding author on reasonable request.

References

1. Polder D, Van Hove M. Theory of radiative heat transfer between closely spaced bodies. Phys Rev B. 1971;4:3303.
2. Loomis JJ, Maris HJ. Theory of heat transfer by evanescent electromagnetic waves. Phys Rev B. 1994;50:18517.
3. Joulain K, Mulet J-P, Marquier F, Carminati R, Greffet J-J. Surface electromagnetic waves thermally excited: radiative heat transfer, coherence properties and Casimir forces revisited in the near field. Surf Sci Rep. 2005;57:59.

4. Rousseau E, Siria A, Jourdan G, Volz S, Comin F, Chevrier J, Greffet J-J. Radiative heat transfer at the nanoscale. Nature Photon. 2009;3:514–7. https://doi.org/10.1038/nphoton.2009.144.
5. Shen S, Narayanaswamy A, Chen G. Surface phonon polaritons mediated energy transfer between nanoscale gaps. Nano Lett. 2009;9:2909.
6. Song B, Thompson D, Fiorino A, Ganjeh Y, Reddy P, Meyhofer E. Radiative heat conductances between dielectric and metallic parallel plates with nanoscale gaps. Nature Nanotech. 2016;11:509–14. https://doi.org/10.1038/nnano.2016.17.
7. Thompson D, Zhu L, Mittapally R, Sadat S, Xing Z, McArdle P, Qazilbash MM, Reddy P, Meyhofer E. Hundred-fold enhancement in far-field radiative heat transfer over the blackbody limit. Nature. 2018;561:216.
8. Luo X, Salihoglu H, Wang Z, Li Z, Kim H, Liu X, Li J, Yu B, Du S, Shen S. Observation of near-field thermal radiation between coplanar nanodevices with subwavelength dimensions. Nano Lett. 2024;24:1502.
9. Tachikawa S, Ordonez-Miranda J, Jalabert L, Wu Y, Anufriev R, Guo Y, Kim B, Fujita H, Volz S, Nomura M. Enhanced far-field thermal radiation through a polaritonic waveguide. Phys Rev Lett. 2024;132: 186904.
10. Huber AJ, Deutsch B, Novotny L, Hillenbrand R. Focusing of surface phonon polaritons. Appl Phys Lett. 2008;92: 203104.
11. Gluchko S, Ordonez-Miranda J, Tranchant L, Antoni T, Volz S. Focusing of surface phonon-polaritons along conical and wedge polar nanostructures. J Appl Phys. 2015;118: 064301.
12. Park I-Y, Kim S, Choi J, Lee D-H, Kim Y-J, Kling MF, Stockman MI, Kim S-W. Plasmonic generation of ultrashort extreme-ultraviolet light pulses. Nature Photon. 2011;5:677.
13. Smirnov V, Stephan S, Westphal M, Emmrich D, Beyer A, Golzhauser A, Lienau C, Silies M. Transmitting surface plasmon polaritons across nanometer-sized gaps by optical near-field coupling. ACS Photonics. 2021;8:832.
14. Ordonez-Miranda J, Tranchant L, Tokunaga T, Kim B, Palpant B, Chalopin Y, Antoni T, Volz S. Anomalous thermal conductivity by surface phonon-polaritons of polar nano thin films due to their asymmetric surrounding media. J Appl Phys. 2013;113: 084311.
15. Basu S, Zhang ZM, Fu CJ. Review of near-field thermal radiation and its application to energy conversion. Int J Energy Res. 2009;33:1203.
16. Rodriguez AW, Reid MTH, Johnson SG. Fluctuating-surface-current formulation of radiative heat transfer: theory and applications. Phys Rev B. 2013;88: 054305.
17. Wu Y, Ordonez-Miranda J, Gluchko S, Anufriev R, Meneses DDS, Campo LD, Volz S. Nomura M Enhanced thermal conduction by surface phonon-polaritons. Sci Adv. 2020;6:eabb4461.
18. Modest MF. Radiative heat transfer. California: Elsevier Science; 2003.
19. Volz S, Ordonez-Miranda J. Heat transport driven by surface electromagnetic waves. Cham: Springer; 2024.
20. Ordonez-Miranda J, Anufriev R, Nomura M, Volz S. Dimensional crossover in thermal radiation: From three- to two-dimensional heat transfer between metallic membranes. Phys Rev Appl. 2024;22:L031006.
21. Tang L, Corrêa LM, Francoeur M, Dames C. Corner- and edge-mode enhancement of near-field radiative heat transfer. Nature. 2024;629:67.